ADVANCED MATERIALS FOR OPTICS AND ELECTRONICS, VOL 5, 19–30 (1995)

IR and UV Laser-assisted Deposition from Titanium Tetrachloride: a Comparative Study

R. Alexandrescu*, R. Cireasa, B. Dragnea, I. Morjan and I. Voicu
Institute of Atomic Physics, PO Box MG-6, Bucharest, Romania

A. Andrei
Institute for Nuclear Reactors, Pitesti, Romania

F. Vasiliu
Research Institute for Aircraft Materials, PO Box 24, Bucharest, Romania

C. Popescu
LACECA Research Center, 95 Siret St., RO-78308 Bucharest, Romaina

Laser-induced $TiCl_4$ decomposition at vapour pressure was performed and comparative study of the composition and structure of thermally (at 10.6 μm) and photolytically (at 248 nm) deposited Ti-based films is presented. Emphasis was given to the less explored titanium deposition process by CO_2 laser pyrolysis of $TiCl_4$. The detailed structure of films deposited on quartz substrates was examined by scanning electron microscopy and X-ray photoelectron spectroscopy. The influence of the incident laser energy on the chemical content of the films as well as on the film growth rate was demonstrated. The results indicate that in the thermal IR decomposition of $TiCl_4$ a multilayer structure is formed with unsaturated $TiSi_x$ at the interface and oxidized phases at the surface. The photolytic process leads to films with increased purity and a specific growth morphology.

KEYWORDS laser photochemistry; LCVD; laser photolysis; laser pyrolysis

INTRODUCTION

Compared with conventional CVD techniques, surface selectivity, lower contamination and rapid film formation may often be achieved in laser-assisted deposition of metallic thin films. The purity of laser-deposited films depends in a critical way on the decomposition chemistry of the vapour phase precursor and on its interaction with the substrate surface.[1]

Titanium and titanium alloys are important technological materials. Often used as thin films or coatings, their rapidly growing applications run from microelectronics and electrochemical fabrication to corrosion-resistant and non-toxic biomedical devices. One of the most commonly used precursors for laser-induced deposition of titanium-based films is titanium(IV) tetrachloride. Using the large absorption cross-section of $TiCl_4$ in the UV range of excimer laser emission, direct writing of titanium lines was achieved photochemically on lithium niobate.[2,3] Deposition of titanium oxide,[4] carbide,[5,6] nitride[7] and silicide[8] by laser thermal decomposition of $TiCl_4$ in the presence of additives ($H_2 + CO_2$, $C_2H_4 + H_2$, CH_4 and $N_2 + H_2$ respectively) showed the advantages of the highly localized heat release and chemical treatment occurring in laser chemical vapour deposition processes. We should note that in most of these papers[2–6] the film purities were not reported; studies on titanium compound layers recently revealed a close correlation between film composition and irradiation parameters.[7–8]

The purpose of this work was twofold: to perform a comparative study on laser-deposited Ti-based layers obtained by $TiCl_4$ photolytic (at

* Authors to whom correspondence should be addressed.

CCC 1057–9257/95/010019–12

Received 28 July 1994
Accepted 27 October 1994

248 nm) and thermal (at 10.6 μm) decomposition and to systematically analyse the potential of the less explored CO_2 laser pyrolysis process. In contrast with previous reports on $TiCl_4$ laser chemistry, the experiments were carried on at $TiCl_4$ vapour pressure in order to approach the practical demands of the thin film industry. In all cases a perpendicular laser beam-quartz substrate configuration was used.

Transmission measurements at various wavelengths were used in order to evaluate the film thickness. The deposited layers were characterized by scanning electron microscopy (SEM) and X-ray photoelectron spectroscopy (XPS).

A modelling process for the kinetics of film growth in both IR and UV $TiCl_4$ irradiation is also proposed which correlates the experimental conditions with the properties of the obtained Ti-based layers.

EXPERIMENTAL

The irradiation of $TiCl_4$ was conducted at room temperature and $TiCl_4$ vapour pressure (~10 Torr) in the static pressure mode. A detailed description of the experimental device can be found in Refs 9 and 10. It consists essentially of a glass reaction cell (base pressure 10^{-3} Torr) into which both the $TiCl_4$ vapour and the quartz substrate are introduced. Either a medium-power CW CO_2 laser (maximum output power 55 W) or a KrF excimer laser (40 mJ/pulse, 10 ns pulse length, 1 Hz repetition frequency) was used. In both cases the laser radiation was in a direction perpendicular to the quartz substrate. In the case of UV irradiation the deposition occurred on the cell front window. The temperatures of the substrate were monitored by means of thermocouples mounted on the back side of the quartz substrate. The recorded overall substrate temperatures varied between 600 and 100 °C.

In order to investigate the changes in film composition induced by different irradiation regimes, the unfocused radiation of the CO_2 laser was sampled by means of an electrical chopper with variable pulse length L_p (ms) and frequency f (Hz) (Table 1). For the irradiation regimes listed in Table 1, an effective irradiation time t was deduced as a cumulative time in which the sample was 'seen' by the laser beam, $t = \tau f L_p$.

In the UV laser experiments the KrF laser beam (1×1.5 cm^2 cross-section) was focused 8 mm in front of the cell entrance window through a 17 cm focal length lens. In order to estimate the dynamics of film growth, increasing numbers of pulses were used (50, 100, 350, 700 and 1500 pulses at constant pulse frequency).

The thickness of the deposited films was measured by interference microscopy ($\frac{1}{20}\lambda_{vis}$ accuracy). The IR transmission measurements were performed in the transparent region of the quartz substrate.

The chemical composition of the films was analysed by electron spectroscopy. Photoelectron spectra were obtained with a VG Escalab MK II spectrometer (base pressure $\sim 9 \times 10^{-10}$ mbar). For XPS, Al Kα radiation ($h\nu = 1486.6$ eV) was used. Spectral calibration was performed by means of the Ag $3d_{5/2}$ ($h\nu = 368.26$ eV) and Ag M_4NN ($h\nu = 1128.78$ eV) lines, with the Fermi level as an energy reference. A 'flood gun' was used for the correction of surface charging with respect to the C ls peak position at 284.6 eV and corresponding linewidths.

The morphology of the deposited films was studied by scanning electron microscopy, which was performed in a Phillips SEM-515 scanning electron microscope operating at 15–25 kV in the secondary electron image mode. In some cases a

Table 1. CO_2 laser irradiation regimes

Laser power P (W)	18	18	18	18	22
Pulse length L_p (ms)	6.3	13.3	13.3	6.25	6.25
Frequency f (Hz)	7.15	7.14	13.3	80	80
Accumulated energy E (J) (after $\tau = 300$ s irradiation time[a])	243	513	955	2700	3300

[a] Cycles of 10 s irradiation time were separated by 5 s shut intervals in order to avoid large temperature gradients in the substrate.

thin carbon film was evaporated on the specimen surfaces to avoid space charge effects.

RESULTS AND DISCUSSION

$TiCl_4$ vapours are strongly adsorbed on all the internal walls of the reaction cell. It was found experimentally that even at 1.5 Torr the average thickness of the $TiCl_4$ adsorbed layer gives a coverage of about 50 layers, which continues to increase with increasing pressure (though not so strongly bonded). A large adsorbed layer close to liquefaction is expected to be formed on the substrate when the vapour pressure is reached.[2] In the UV wavelength range the radiation is absorbed by $TiCl_4$ (the vapour phase absorption cross-section of $TiCl_4$ at 248 nm is about 3×10^{-18} cm^2).[2] The 4.98 eV photon energy could break a Ti•Cl bond (4.47 eV bonding energy).[3] It should also be noted that in our experimental arrangement the photolysis of the adsorbed $TiCl_4$ layer was favoured over a competing gas phase photochemistry. In the IR wavelength range $TiCl_4$ is transparent to the laser radiation and the film grows through the thermal decomposition of reactant molecules adsorbed on the laser-heated surface. In both cases there is a constant renewal of the $TiCl_4$ layer during film growth, which is assured by diffusive mass transport processes.[1]

The variation in film thickness with increasing effective irradiation time is displayed in Fig. 1(a) for the film grown at 10.6 μm and in Fig. 1(*b*) for the photolytic UV deposition. The plots were obtained by combining the results of IR transmission measurements with those given by the interferential microscopy method (the error bars take into account the limitations of this method). In the IR irradiation regime (Fig. 1(a)) the film thickness varies from 550 Å after 5 s irradiation time to about 1250 Å after 150 s. Accordingly, the deposition rate decreases from 14 to 2.5 Å s^{-1} respectively. From Fig. 1(b) one may observe that the UV photolytic process is much more effective in inducing $TiCl_4$ decomposition and subsequent film growth. A film thickness of more than 2000 Å could be reached in fewer than $N = 1500$ pulses (less than 1 ms effective irradiation time). A further increase in exposure time ($N > 1500$ pulses) led to a spreading of the deposit (photoablation) and a consequent decrease in film thickness.

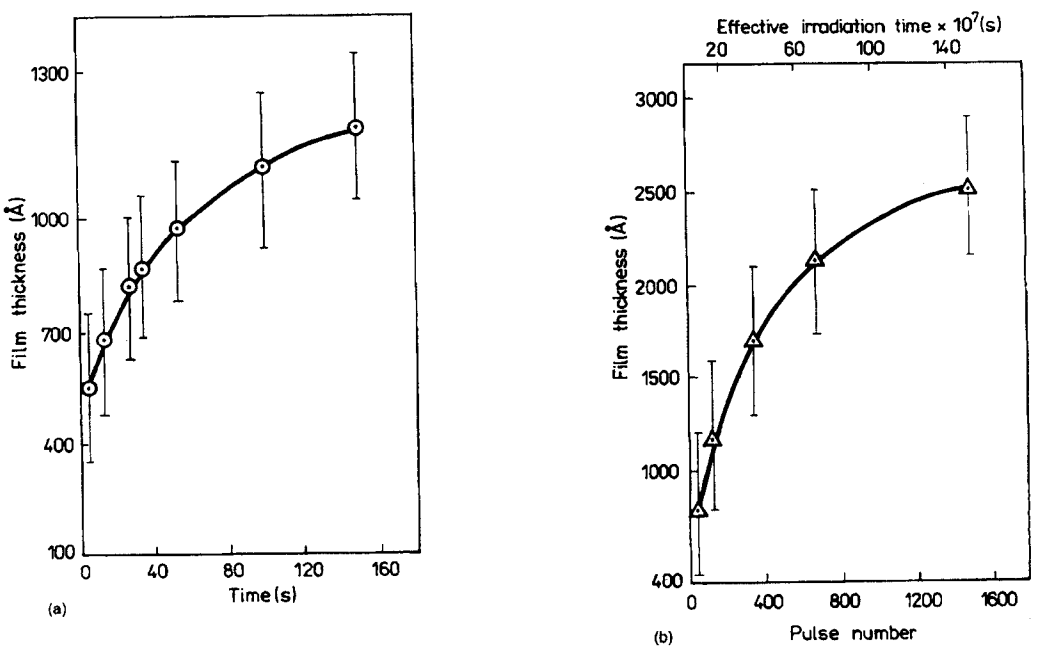

Fig. 1. Film thickness vs. effective irradiation time (and number of UV pulses): (a) CO_2 laser; (b) KrF laser (thickness measured in central part of irradiated area)

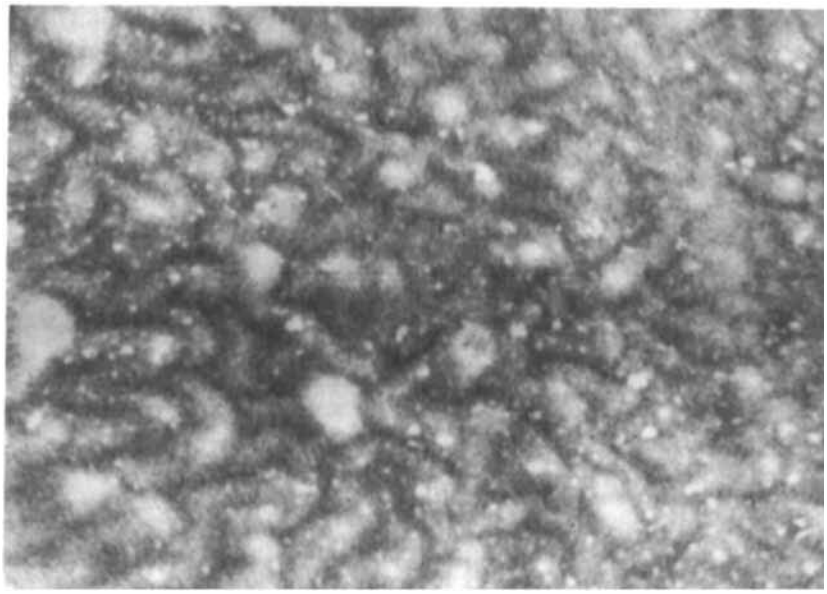

(a)

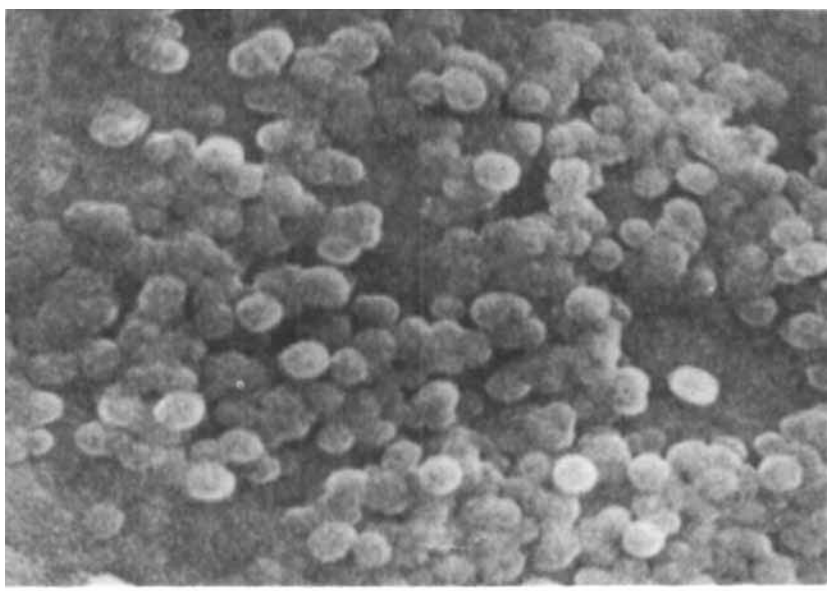

(b)

Fig. 2. Scanning electron micrographs of films obtained at different wavelengths of laser-induced deposition process: (a) 10.6 μm, 243 J accumulated laser energy (3000×); (b) same film as in (a) but at higher magnification (10,000×); (c) 248 nm, 50 laser pulses (3000×), central part of irradiated area; (d) 248 nm, 50 laser pulses (3000×), external part of irradiated area

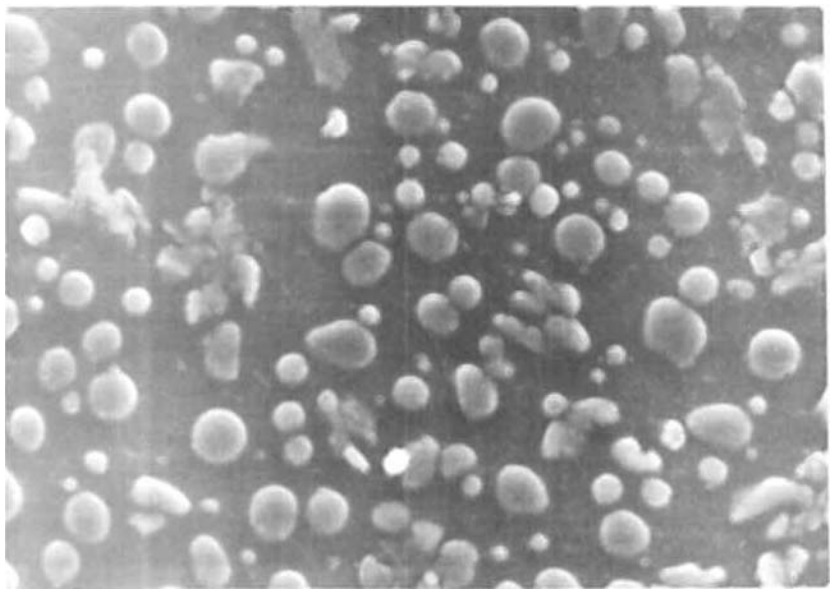

(c)

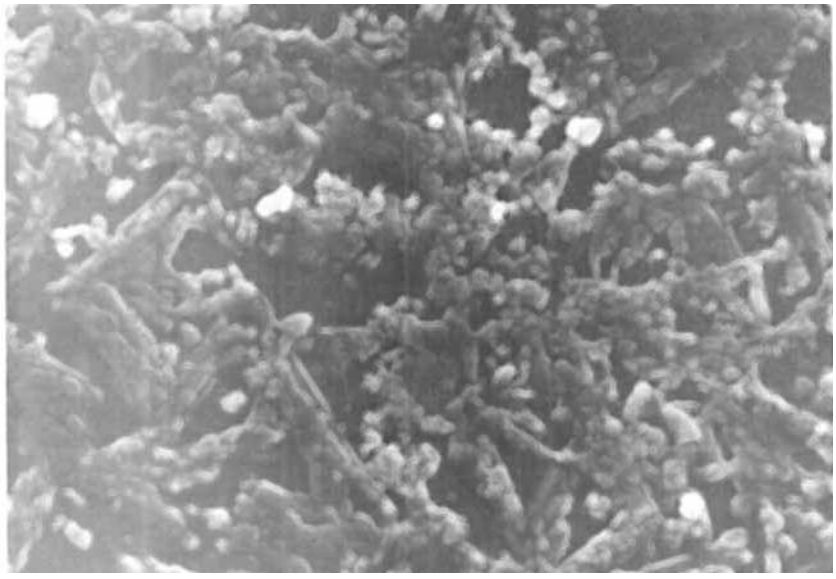

(d)

Fig. 2. *Continued*

Scanning electron micrographs showed an essential difference in the nucleation and growth of films deposited at 10.6 μm and 248 nm (Fig. 2). The film grown by pyrolytic surface reaction exhibited a rather smooth surface with a uniform grain refined microstructure even at low incident energies (242 J in Fig. 2(a)). At increased magnification a quasi-spherical appearance of the agglomerates is revealed (Fig. 2(b)). The film obtained by photochemical $TiCl_4$ decomposition with a small number of laser pulses showed a discontinuous film growth in which large droplets emerged in the central region of irradiation (Fig. 2(c); film obtained with 50 UV pulses). Around the solidified 'droplet' region the film showed a dendritic growth with randomly oriented 'channels' filled with more irregular, small particles (Fig. 2(d)). We may note that the contribution of a gas phase chemistry to the morphology of the UV-deposited films (Figs 2(c) and 2(d)) is unlikely owing to (i) the geometry of irradiation, in which the $TiCl_4$ adsorbed layer was interposed between the quartz substrate and vapours, and (ii) the absence of a powdery deposit (presumably $TiCl_3$ species), which would be observed if gas phase reactions at high pressures were involved.[2] On the other hand, a non-uniform energy distribution over the cross-section of the KrF laser beam (which was observed experimentally) could induce small local differences in the temperature rise of the substrate, imposing different trends on the mechanisms of aggregation and film growth. The grain size distribution (as revealed by three micrographs of the type presented in Fig. 2(c)) is shown in Fig. 3 together with the calculated dependence $n = CR^{\alpha}$, where R is the droplet radius, C is a fitting constant and $\alpha = -0.6$. It may be observed that the real distribution (obtained for 200 particles) agrees well with this dependence, which is characteristic of systems with autosimilarity.[11] Models of the growth of aggregates in such systems show the formation of relatively compact clusters whose density correlations are independent of the distance between occupied sites. In contrast, the dendritic film growth revealed in the micrograph of Fig. 2(d) seems to point to a diffusion-limited aggregation (DLA) mechanism in which surface diffusion and cluster–cluster aggregation play the main role.

The XPS technique was used in order to determine the chemical composition of films obtained by irradiation at 10.6 μm and 248 nm as well as the evolution of film composition with increasing

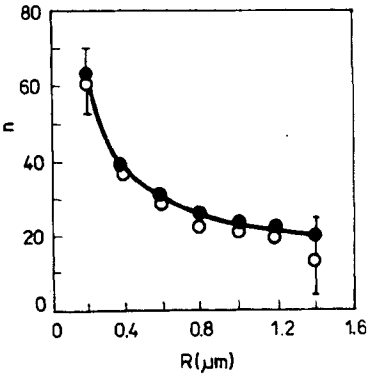

Fig. 3. Grain size distributions: obtained ∘, from micrographs; •, from calculated dependence $n = cR^{\alpha}$ ($\alpha = -0.6$; see text). The extreme points on the curve are marked with the calculated error bars

incident (accumulated) laser energy. Using a deconvolution technique ('peak synthesis'), the analysis of chemical states in films obtained under different irradiation conditions was performed. For each chemical state the Ti 2p level spectrum exhibits a double structure. Owing to the overlap of many neighbouring peaks in an energy gap of a few electronvolts, careful evaluation of the different contributions to the spectral Ti 2p region was needed. Binding energy (BE) peak positions and FWHM values were chosen according to literature data[12,13] by imposing a correct ratio between the areas of the two Ti doublet components.

Besides the hydrocarbonated C contribution, the chemical composition of the surface layers of deposited films included titanium, oxygen and various quantities of silicon. Unless special reference is made, the reported Si and O quantities in UV films were obtained after subtraction of the quartz substrate signal. It is important to note that within the limits of the technique the presence of chlorine has not been revealed. Earlier studies[3] performed at even lower UV laser energies have also noted the efficient elimination of Cl from the growing layer (Cl < 2 at.%), which was attributed to thermal desorption processes.

The evolution of total Ti and Si contents of deposited films with increasing incident laser energy is presented in Figs 4(a) and 4(b) for the CO_2 and excimer laser-induced reactions respectively. The following differences may be observed: (i) there is a rapid and rather steep increase in Ti content in the UV process, reflecting a densification of the superficial layer with laser energy accumulation; (ii) there is a decrease in the

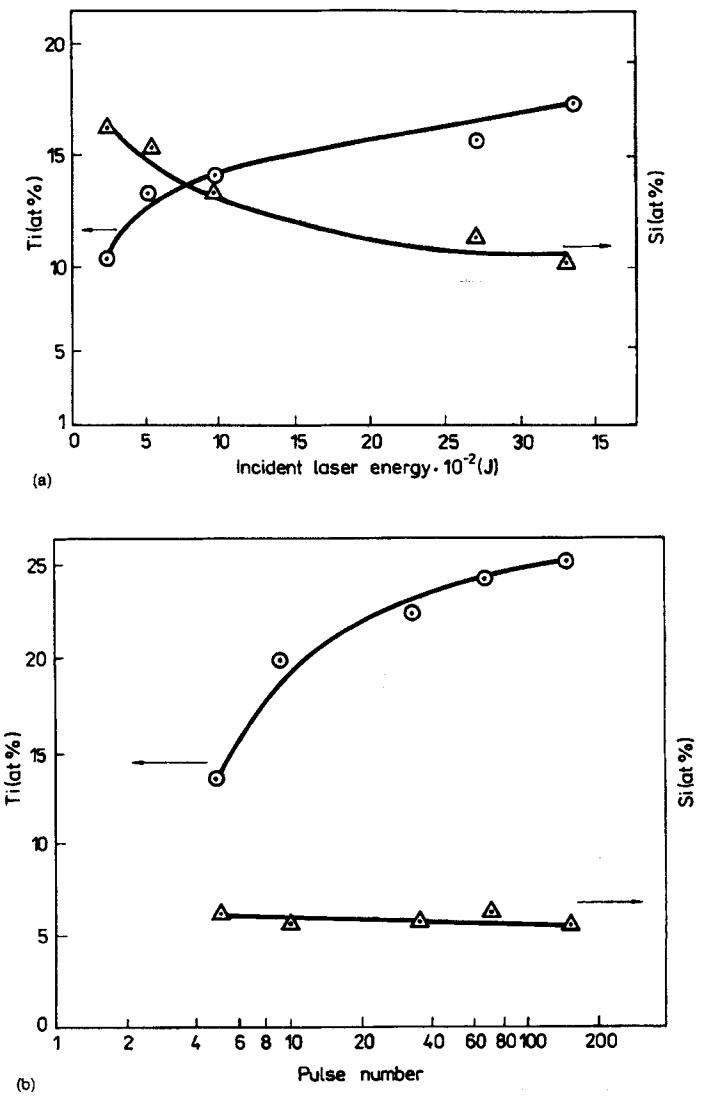

Fig. 4. XPS results for evolution of total Ti (○) and Si (Δ) contents (a) with increasing accumulated incident energy of CO_2 laser and (b) with increasing numbers of pulses of UV laser radiation. The curves between points are merely a guide for the eye

Si content of surface layers in the IR pyrolytic deposition, while in the UV process the Si content keeps approximately constant at a rather low value.

In Table 2 data on the concentrations of silicon and oxygen relative to titanium in samples obtained at various laser energies in both irradiation regimes are presented. The data are reported as $x_i/(x_{Ti}+x_i)$,[5] where x_i and x_{Ti} refer to the peak-to-peak amplitudes of the photoelectron signal for the contaminant (i=O, Si) and titanium respectively.

It has been shown[14–17] that at elevated temperatures (exceeding 800 °C) a reaction between Ti and SiO_2 takes place, resulting in a multilayer structure with interfacial mixing of the dominant titanium silicide at the SiO_2 interface and graded titanium oxidized phases at the surface. Particularly in the CO_2 laser irradiation, a thickening of the oxidized Ti films deposited on quartz substrates was observed, together with a lowered contribution from the Ti–Si layer[9] (as deduced also from Fig. 4).

Table 2. Titanium, oxygen and silicon surface composition of films as determined by X-ray photoelectron spectroscopy

Irradiation at 10.6 μm			Irradiation at 248 n		
Accumulated laser energy (J)	$(x_O/(x_{Ti}+x_O)$	$x_{Si}/(x_{Ti}+x_{Si})$	Accumulated laser energy (J)	$x_O/(x_{Ti}+x_O)$	$x_{Si}/(x_{Ti}+x_{Si})$
243	0.88	0.63	0.3	0.83	0.96
513	0.84	0.54	6	0.79	0.77
955	0.84	0.48	21	0.76	0.80
2700	0.82	0.37	42	0.74	0.79
3300	0.80	0.31	90.	0.73	0.825

[a] After 300 s irradiation time.

Figure 5 displays the typical structure of the Ti 2p line for samples obtained by the pyrolytic reaction of $TiCl_4$ at various CO_2 laser energies. The main peak, which for sample 'a' (deposited at 513 J laser energy) lies around 457.4 eV· is associated with an oxidized Ti state corresponding to a sub-TiO_2 valence.[18,19] With increasing laser energy this peak is shifted slightly towards higher BE values (the peak of curve 'd' in Fig. 5 lies around 457.8 eV), indicating a nearly stoichiometric TiO_2 formation. At the same time there is a narrowing of the line shape, pointing to a diminished contribution of intermediate oxidized species TiO_x, $x<2$, which interfere at the low-energy side of the Ti 2p line curve. According to literature data,[12] a contribution of $TiSi_x$ species also lies on the low-energy side of the Ti 2p line, with binding energy close to (but lower than) the oxidized TiO_x phases. Using the peak synthesis technique, TiO_2, TiO_x and $TiSi_x$ contributions for sample 'a' in Fig. 5 are evidenced at 458, 457.1 and 455.7 eV respectively (Fig. 6).

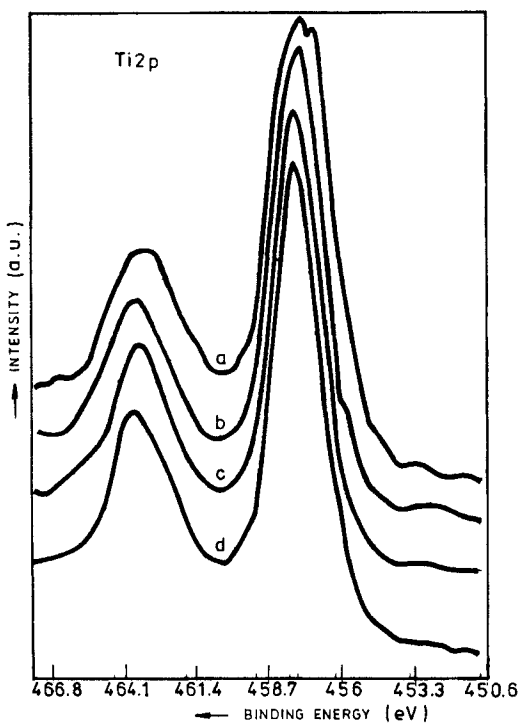

Fig. 5. XPS spectra for Ti 2p line. The samples were obtained by CO_2 laser irradiation at energies of (a) 513 J, (b) 955 J, (c) 2700 J and (d) 3300 J

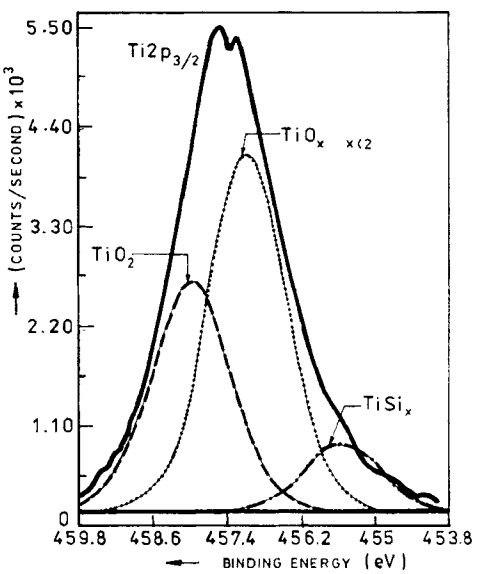

Fig. 6. Ti $2p_{3/2}$ line and its deconvolution for film grown under CO_2 laser irradiation (at 513 J incident laser energy). The three components are attributed to TiO_2 (458 eV), TiO_x, $x<2$ (457.1 eV), and $TiSi_x$ (455.7 eV)

There is a lower $TiSi_x$ contribution in the Ti 2p line spectra of UV films (Fig. 7) which grows slightly with increasing number of laser pulses (from curve 'b' at 700 laser pulses to curve 'a' at 1500 laser pulses). We should observe that in films obtained by UV photolysis a contribution from elemental Ti towards 454 eV is noticeable (curve 'a' in Fig. 7).

The Si 2p line spectra of films deposited at various laser energies (indicated in Table 2) show that in the IR pyrolytic process a prevailing single structure appears at 99.6 eV (Fig. 8, curve 'a') which may be attributed to Si bound in $TiSi_x$.[18] At high power densities ($p > 55$ W) local damage of the substrate occurred and the Si 2p line was characterised by a double structure where the Si—O bond in SiO_2 appeared.[9] In this respect it is worthwhile to note that silicon (either bound to Ti or in elemental form) diffusion towards the surface has already been detected by backscattering[15] and in Auger[18] and XPS[17] depth profiles of annealed Ti on SiO_2. The Si 2p line in UV films (Fig. 8, curve 'b', $N = 700$ pulses) was analysed by the peak synthesis technique. Owing to non-uniform film growth, a contribution from the quartz substrate is obvious (the Si—O bond at about 102.2 eV, curve 1), together with elemental Si (BE ≈ 100.4 eV, curve 2) and Si bound to Ti (BE ≈ 99.8 eV, curve 3).[18]

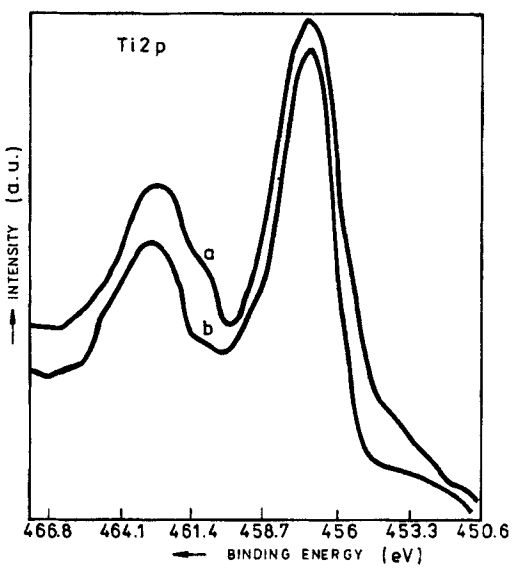

Fig. 7. Ti 2p line spectra for film obtained by UV laser irradiation with (a) 1500 laser pulses and (b) 700 pulses

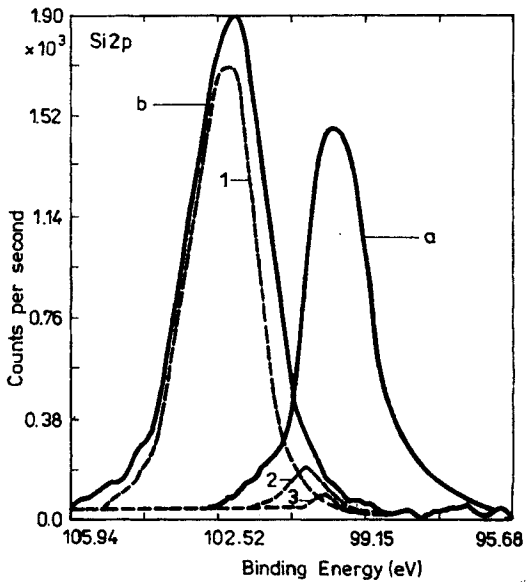

Fig. 8. Si 2p line spectra for surface of films obtained during two irradiation regimes: (a) IR radiation (200 J incident laser energy) — peak corresponds to prevailing $TiSi_x$ composition (99.6 eV); (b) UV radiation (350 pulses) — peak deconvolution technique indicates, besides substrate (SiO_2) contribution (broken curve 1), possible presence of elemental Si and $TiSi_x$ (dotted curves 2 and 3 respectively)

The composition of oxidized layers in thin titanium films (either natural or synthesized by various methods) has been the subject of many papers.[15,17–21] It is well known that titanium films are extremely reactive to oxygen both during deposition and after exposure to ambient atmosphere. A comparative study of the oxidation states of films grown in IR and UV processes may be followed in Figs. 9 and 10, where a superposition of O 1s line spectra for samples obtained by IR (Fig. 9, curve 'a') and UV (Fig. 9, curves 'b' and 'c') is presented. Upon irradiating adsorbed $TiCl_4$ layers at 10.6 μm, a double-peak structure appears in which the peak at 530.2 eV (curve 1 in Fig. 9) can be attributed to surface-oxidized titanium species. Further contributions from chemisorbed oxygen (at 532.5 eV, curve 2) and hydroxy groups (at 530.8 eV, curve 3) are also noticeable.

It is interesting to note a quite different evolution of oxygen content of films deposited by UV photolysis. At a reduced pulse number ($N = 100$, Fig. 9, curve 'b') most of the O content is provided by chemisorbed oxygen. With an increased number of pulses ($N = 1500$, Fig. 9, curve 'c')

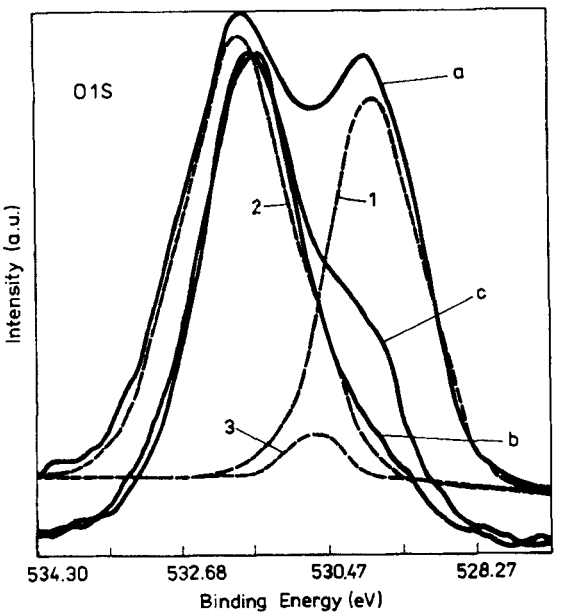

Fig. 9. Superposition of O 1s line spectra for films obtained (a) by CO_2 laser irradiation (955 J incident energy), showing deconvoluted curves 1, 2 and 3 (for oxidized Ti species and chemisorbed oxygen and hydroxy groups respectively), (b) by excimer laser irradiation with 100 pulses and (c) by excimer laser irradiation with 1500 pulses

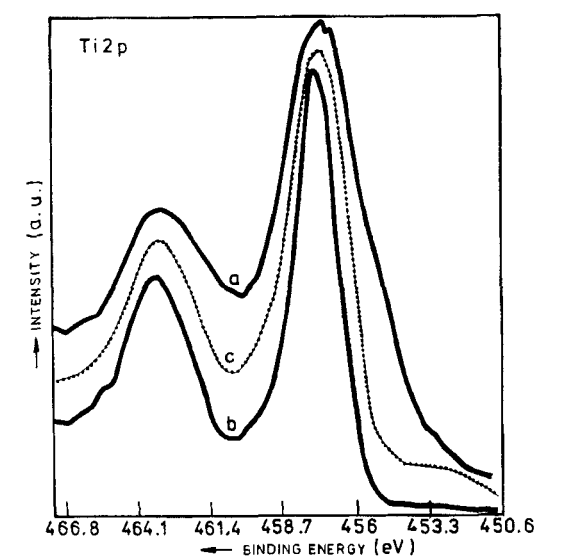

Fig. 10. Superposition of Ti 2p line spectra for films deposited (a) at 243 J CO_2 laser energy, (b) at 2700 J CO_2 laser energy and (c) with 1500 pulses of KrF excimer laser

there is a marked increase in O bonds in TiO_x (the shoulder observed in curve 'c' at about 530 eV), but without reaching the quantity and stoichiometry of the IR-oxidized films (where nearly stoichiometric TiO_2 formation was observed; see Fig. 5). Further support for this interpretation is found in Fig. 10, where a comparison between the Ti 2p line spectra of films deposited at two extreme CO_2 laser energies (curve 'a', 243 J; curve 'b', 2700 J) and the film deposited at the maximum UV laser energy (curve c, $N = 1500$ laser pulses) is presented. With increasing laser energy the Ti 2p line in the IR process narrows, showing a decreased contribution of suboxide phases (see also Fig. 5), while in the excimer laser deposition process the prevailing TiO_x phases are still detected (appearing towards lower BE values).

For an interpretation of the XPS data on surface analysis, one should keep in mind that information is obtained from a depth region of about 60 Å (the inelastic mean free path of electrons in titanium oxide is 15–18 Å[12]).

A modelling of the processes occurring in both IR and UV laser decomposition of $TiCl_4$ at vapour pressure and of the dynamics of film growth on a quartz substrate with increasing laser energy should be consistent with the evolutions of chemical composition and structure of the deposited films. The CO_2 laser radiation is driving a purely thermal process where in the first phase titanium may be formed by local heating and subsequent thermal decomposition of $TiCl_4$ adsorbed on the surface (decomposition of $TiCl_4$ was observed at 600 °C; see Ref. 3 and references cited therein):

$$TiCl_4 \rightarrow Ti + 2Cl_2 \qquad 1$$

The contact of freshly formed Ti with the quartz substrate at temperatures above 700 °C could lead to bond breakage of the SiO in SiO_2 by a redox-type reaction in which the metal is oxidized while the quartz is reduced:[4]

$$11Ti + 3SiO_2 \rightarrow Ti_5Si_3 + 6TiO \qquad 2$$

In Eqn. 2 the metal-rich silicide and TiO are likely to be formed as an intermediate layer at the Ti–SiO_2 interface owing to the lack of Si and O atoms in comparison with Ti atoms.[16] Alternatively, the reduction of SiO_2 is liberating oxygen which diffuses in the Ti layer and forms graded oxidized phases from TiO_x ($x < 2$) to nearly stoichiometric TiO_2 towards the surface. It has

been shown[18] that though to a lesser extent, silicon is also diffusing, probably reacting with Ti–O to give $TiSi_x$ which in low concentration extends up to the surface (Figs. 4(a) and 6). As the film grows, changes in the kinetics of film formation are detected. The decrease in the $TiSi_x$ component (observed in Figs. 4(a) and 5) may be due to a thicker interfacial Ti_5Si_x layer which could screen the quartz substrate from direct titanium contact. At the same time an increased contribution from heavily oxidized titanium species at the surface (Fig. 5) is observed: an induced decomposition of oxygen-deficient TiO_x compounds in the presence of titanium at about 400 °C was supposed[20] which could provide adequate oxygen to produce a more stoichiometric TiO_2 layer. We may thus note that in the IR irradiation process the film oxidation seems to be primarily the result of the deposition process itself.

In the UV irradiation the KrF excimer laser radiation should induce photolytic decomposition of the adsorbed $TiCl_4$ layer by an overall reaction[3]

$$TiCl_4(\text{adsorbed}) \rightarrow Ti(s) + 2Cl_2(g) \qquad 3$$

It was observed[2] that reaction 3 is specific for an autocatalytic surface photochemistry of $TiCl_4$, because in the gas phase the successive dechlorination towards pure Ti was not found and the reaction stopped after the removal of one Cl atom and the production of $TiCl_3$. With an increased number of pulses there is the freshly formed titanium that further catalyses the deposition, mainly by strongly absorbing the UV radiation (an absorption coefficient $\alpha = 5.4 \times 10^5\ cm^{-2}$ at 248 nm was determined[3]) and subsequent local heating of the already formed deposit (temperatures exceeding 600 °C necessary to thermally decompose $TiCl_4$ or partially chlorinated species were estimated.[2,3]). Once the primary Ti nuclei are formed at the interface, the film experiences an accelerated growth.

A two-stage-like process[3] is thus developing in the UV deposition: (i) primary Ti nuclei are formed by photolytic $TiCl_4$ dechlorination on the surface (Eqn. 3), which is further catalysed by seeds of freshly formed titanium; (ii) the increased absorption of the UV quanta enhanced by the metal deposit induces a local temperature increase which in turn leads to incipient redox reactions such as Eqn. 2 (favoured by film discontinuities). Consequently, the UV film composition is still showing traces of Si and $TiSi_x$ species, but elemental Ti is appearing together with a suboxide stoichiometry (TiO_x, $x < 2$) of surface layers (obviously as an effect of the ambient atmospheric exposure).

CONCLUSIONS

This study was performed in order to comparatively elucidate the different degrees of purities obtained in Ti film deposition processes by IR and UV laser decomposition of $TiCl_4$ at normal vapour pressure when a perpendicular geometry of irradiation and quartz substrates are used. In both cases the structure and film composition were analysed, which could provide useful information for further rigorous applications. The experiments run at $TiCl_4$ vapour pressure as well as titanium film formation with the help of a CW CO_2 laser could be first attempts at a systematic study.

The results showed that films grown in CO_2 laser-induced processes are smoother and more compact than photolytically obtained films. Their chemical composition is also different as compared with those obtained by UV mechanisms. The occurrences of reactions 1 and 2 could account for the quite large amount of $TiSi_x$ and nearly stoichiometric TiO_2 found in the films. The films obtained by excimer laser irradiation of adsorbed $TiCl_4$ have essentially a droplet-like morphology which seems to obey an autosimilarity law of aggregation. The chemical composition exhibits elemental Ti and a much lower amount of $TiSi_x$, while their oxidized surface phases remain in suboxide form.

A thermal mechanism is assumed to be responsible for the formation of the IR-deposited films, while for the UV film formation a photolytic mechanism can be ascribed for the beginning of the process and a thermal one overlaps thereafter. A deeper kinetic theory modelling these findings will be developed in a future work.

ACKNOWLEDGEMENTS

We would like to thank Dr C. Grigoriu from the Institute of Atomic Physics, Bucharest for his valuable assistance with the KrF excimer laser irradiation.

REFERENCES

1. T. H. Baum and P.B. Comita, *Thin Solid Films*, 1992, **218**, 80.
2. J. Y. Tsao, R. A. Becker, D. J. Ehrlich and F. J. Loenberger, *Appl. Phys. Lett.*, 1983, **42**, 558.
3. C. Lavoie, M. Meunier, S. Boivin, R. Isquierdo and P. Desjardins, *J. Appl. Phys.*, 1991, **70**, 2343; *Appl. Phys. A*, 1991, **53**, 339.
4. S. D. Allen, *J. Appl. Phys.*, 1981, **52**, 6501.
5. /J. H. Westberg, M. Boman and J. O. Carlsson, *Thin Solid Films*, 1992, **218**, 8.
6. M. L. E. Paramès and O. Conde, *J. Physique IV, Colloq. C3*, 1993, **3**, 217.
7. Y. H. Croonen and G. Verspui, *J. Physique IV, Colloq. C3*, 1993, **3**, 209.
8. H. Westberg, M. Boman and J. O. Carlsson, *J. Physique IV, Colloq. C3*, 193, **3**, 225.
9. R. Alexandrescu, R. Cireasa, B. Dragnea, I. Morjan, I. Voicu and A. Andrei, *J. Physique IV, Colloq. C3*, 1993, **3**, 265.
10. R. Alexandrescu, A. Andrei, I. Morjan, S. Mulenko, M. Stoica and I. Voicu, *Thin Solid Films*, 1993, *218*, 68.
11. T. Viksek (ed), *Fractal Growth Phenomena*, World Scientific Press, New York, 1989.
12. D. Briggs and M. P. Seah (eds.), *Practical Surface Analysis*, Vol. 1, *Auger and X-ray Photoelectron Spectroscopy*, Wiley, Chichester, 1990.
13. T. Chondhury, S.O. Saied, J. L. Sullivan and A. M. Albot, *J. Phys. D: Appl. Phys.*, 1989, **22**, 1185.
14. S. L. Sung, J. Y. Chee and E. W. Merrill, *Ceram. Trans. (Ceram. Thin Thick Films)*, 1990, **11**, 153.
15. J. S. Maa, C. J. Lin and Y. C. Liu, *Thin Solid Films*, 1979, **64**, 439.
16. C. C. Hsu, Y.-X. Wang, S.-D. Yin, B.-Q. Li, M.-J. Ji and J.£X. Wu, *J. Vac. Sci. Technol. A*, 198[illegible], **5**, 1402.
17. C. P. Lofton and W. E. Swartz, *Thin Solid Films*, 1978, **52**, 271.
18. H. Bender, W. D. Chen, J. Portillo, L. Van den Hove, W. Van Der Hove and V. Vandervorst, *Appl. Surf. Sci.*, 1989, **38**, 37.
19. J. Lausmaa, B. Kasemo, H. Mattson and H. Odelius, *Appl. Surf. Sci.*, 1990, **45**, 189.
20. A. R. Nyalosh, E. L. Garvin, F. K. King and R. E. Kirby, *J. Vac. Sci. Technol. A*, 1986, **4**, 2356.
21. C. Ernsberger, J. Nickerson, A. E. Miller, and J. Moulder, *J. Vac. Sci. Technol. A*, 1985, **3**, 2415.